ACS OMEGA

http://pubs.acs.org/journal/acsodf

Article

Optimization of the Sound Absorption Coefficient (SAC) from Cellulose−Silica Aerogel Using the Box−Behnken Design

S. Silviana,* Enggar C. Prastiti, Ferry Hermawan, and Agus Setyawan

Cite This: *ACS Omega* 2022, 7, 41968−41980

Read Online

ACCESS | Metrics & More | Article Recommendations

ABSTRACT: Noise pollution, which has become a major environmental issue in urban areas, can be minimized using acoustic insulation derived from cellulose−silica aerogel. The raw materials required in the process include waste newspaper-based cellulose, geothermal silica, and NaOH/ZnO solution. Therefore, this study investigates the effect of cellulose, silica, and ZnO concentrations on optimizing the sound absorption coefficient (SAC) using the Box−Behnken design (BBD). The results showed that the optimum conditions were obtained at 39.8578 wt % cellulose, 16.5428 wt % silica, and 0.5684 wt % ZnO. The impedance test for the cellulose aerogel and cellulose−silica aerogel showed SAC values of 0.59 and 0.70, respectively, and were characterized by XRD, FTIR, BET−BJH, SEM−EDX, and TG. The results of XRD and FTIR data indicate that the product was cellulose−silica aerogel, and the SEM micrographs showed that silica particles were attached to the fiber surface. Furthermore, type IV isotherms were observed in the cellulose−silica aerogel, typical of mesoporous materials. The presence of silica strengthened the aerogel structure, improved its thermal stability, and increased the surface area but decreased its pore size.

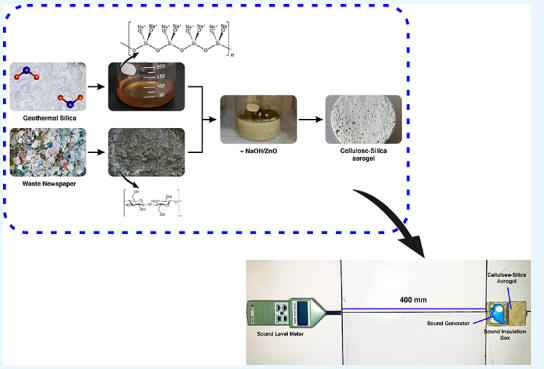

INTRODUCTION

Housing development in urban areas has increased rapidly due to population and infrastructural growth. It generates noise, thereby decreasing the exigencies for citizens' comfort. Furthermore, noise causes permanent hearing loss, unpleasantness, stress, cardiovascular system disease, diabetes, hypertension, and other health issues in humans[1−3] and can be reduced using noise barriers, enclosures, and absorption materials.[4,5] Acoustic insulation made from petroleum such as fiberglass,[6] polyester,[7] polypropylene,[8] polyurethane foam,[9,10] and melamine foam[11] is one of the most effective ways to reducing noise.[12] However, these materials are difficult to recycle, and burning them releases carbon dioxide, methane, and nitrous oxide into the atmosphere.[13] Therefore, there is a need for economical and sustainable acoustic insulation.[14]

Biomass such as cellulose matrix is used as an alternative material for acoustic insulation. Meanwhile, cellulose is the most abundant organic polymer on earth, with unique biodegradability, sustainability, eco-compatibility, and recyclability properties.[15,16] It is derived from waste newspaper,[17−19] cotton,[20] flax,[21] corn,[22] and rice straw.[23−26] The waste newspaper contains about 61% cellulose, 16% hemicellulose, and other inorganic fillers.[27] The high cellulose content indicates its potential as an alternative source for cellulose production.[28] However, the organic compound has limited fire thermal resistance.[29] Therefore, a more environmentally friendly cellulose-based material, such as cellulose aerogel, was developed.[30,31]

Cellulose aerogel is a highly porous material composed of biodegradable fibers with a relatively large surface area of approximately 400 m^2/g when supercritically dried and 100−200 m^2/g in freeze-drying.[32] However, in a few cases, it has a surface area ranging from 2 to 5 m^2/g[33] and a low thermal conductivity between 0.029 and 0.032 W/mK.[34] The mechanical strength of cellulose aerogels manufactured from recycled fibers is lower than that of natural cellulose fibers.[34,35] Therefore, it is necessary to improve the mechanical strength of recycled cellulose by adding a super insulating material such as silica aerogel.[35,36]

Silica aerogel is a lightweight, nanostructured, and highly porous material.[37] It has a low thermal conductivity ranging from 0.015 to 0.025 W/mK[38] and ultralow density similar to that of air,[39] which is 0.00129 g/cm^3. Therefore, it is used as a catalyst,[40] adsorbent,[41] thermal insulation,[42] and acoustic insulation.[35] Furthermore, silica aerogel consists of more

Received: June 15, 2022
Accepted: October 26, 2022
Published: November 10, 2022

than 90% air and less than 10% solid silica by volume.[43] It is released from the geothermal power plant in Dieng.[44] The geothermal silica is widely used in various applications, such as an adsorbent,[45] chitosan coating,[46] preparation of silicon,[47] synthesis of silica xerogel,[48] synthesis of silica aerogel,[49] synthesis of mesoporous silica,[50,51] and superhydrophobic coating.[52] Meanwhile, fly ash,[53] bamboo leaves,[54,55] rice husks,[24,56,57] and bagasse were extensively studied for their silica content.

The initial method for preparing cellulose−silica aerogel is dissolution that is performed using cellulose solvents, such as calcium thiocyanate,[58] ammonium thiocyanate,[59] liquid ammonia/ammonium thiocyanate (NH_3/NH_4SCN),[60] and *N*,*N*-dimethylacetamide/lithium chloride (DMAc/LiCl).[61] However, these solvents are unaffordable, limited to laboratory scale, and mostly cause serious environmental problems.[62,63] Therefore, new eco-friendly cellulose solvents were recently developed, such as the NaOH solution.[64,65] This solvent system is confined to low-molecular-weight cellulose; hence, some additives such as zinc oxide (ZnO) are added to enhance the solubility of the NaOH solution.[63]

Several studies have been conducted regarding the synthesis of cellulose−silica aerogel using supercritical drying[39,66,67] to preserve the porous structure and produce a flexible and translucent cellulose−silica aerogel.[39] However, this process necessitates the use of a high-pressure vessel, which requires expensive equipment.[30] In another study, freeze-drying was employed to synthesize cellulose−silica aerogel.[68] This method can damage the nanostructured gels because it generates crystal growth and development of stress in the pores, possibly leading to fracture of the matrix.[69] Additionally, an extended aging period is necessary to stabilize the gel network, which necessitates using a solvent with a high sublimation pressure and a low expansion coefficient.[70] Therefore, ambient pressure drying is a promising technology used for large-scale industrial applications.[71,72]

Demilecamps et al.[66] prepared cellulose−silica composite aerogels by a one-pot synthesis method. The result showed that the gelation time was reduced by adding sodium silicate to the cellulose−NaOH solution even in the existence of ZnO, which is known as an additive that delays cellulose's gelation. However, the existence of silica decreases the specific surface area. Additionally, He et al.[68] studied the in situ synthesis of cellulose−silica aerogel by one-step impregnation. It was discovered that impregnating the silica particles into the cellulose matrix increases the mechanical properties and specific surface area. Feng et al.[35] analyzed the synthesis of silica−cellulose aerogels from regenerated cellulose fiber and silica precursor methoxytrimethylsilane (MTMS). The results showed good thermal and acoustic insulation properties. The sound absorption coefficients (SACs) of the silica−cellulose aerogels lie between 0.39 and 0.50, which are better than those of cellulose aerogels (0.30−0.40). Furthermore, the synthesis of a silica−cellulose aerogel composite from waste newspaper-based cellulose, silica from geothermal solid waste, and NaOH/PEG solution for acoustic insulation materials has been investigated using a central composite design (CCD) method by Silviana et al.[73] The optimization result showed the optimum point at 1.78 w/v % PEG and 25 wt % cellulose releasing a maximum SAC value of 0.9896.

This study prepared cellulose−silica aerogels using cellulose from waste newspaper, geothermal silica, NaOH/ZnO solution, and ambient pressure drying. The method used to obtain the optimal cellulose, silica, and ZnO concentrations is the Box−Behnken design (BBD), which has fewer experimental trials than other methods.[74] Furthermore, BBD does not combine all factors at the highest or lowest levels at the same time; hence, it is effective in avoiding experiments under extreme conditions, which may lead to undesirable results.[75] The morphological structure and acoustic insulation properties of the aerogel were further investigated.

RESULT AND DISCUSSION

Effect of Cellulose, Silica, and ZnO on the SAC Value.

Table 1 shows the design experiment and SAC values. The specific compositions are listed in Table 6. The optimum result was obtained at a concentration of 35 wt % cellulose, 15 wt % silica, and 1 wt % ZnO with an SAC value of 0.9653. Based on the above, the Design Expert program suggested the quadratic model. Furthermore, the interaction between variables was analyzed using analysis of variance (ANOVA), as shown in Table 2. The parameters *F* value, *p* value, R^2, adjusted R^2, and adequate precision were used to check the model adequacies.

Table 1. The Design Experiment and SAC Value

run	cellulose	silica	ZnO	SAC
1	−1	0	−1	0.9276
2	0	1	1	0.9589
3	0	1	−1	0.9532
4	0	0	0	0.9653
5	−1	0	1	0.9666
6	1	0	−1	0.9758
7	1	0	1	0.9369
8	1	1	0	0.9596
9	1	−1	0	0.9416
10	−1	1	0	0.9359
11	0	−1	−1	0.9374
12	0	−1	1	0.9518
13	−1	−1	0	0.9297

As shown in Table 2, a *p* value less than 0.05 indicates that the corresponding model terms are significant, including A, B, AC, A^2, and B^2. There is only a 2.52% chance of a large *F* value, and it could occur due to noise in the experiment; hence, the signal-to-noise ratio was measured using adequate precision of

Table 2. ANOVA for the Cellulose−Silica Aerogel

source	sum of squares	df	mean square	*F* value	*p* value
model	0.0027	9	0.0003	14.39	0.0252
A: cellulose	0.0004	1	0.0004	19.04	0.0223
B: silica	0.0003	1	0.0003	13.09	0.0363
C: ZnO	0.0001	1	0.0001	3.09	0.1768
AB	0.0000	1	0.0000	1.64	0.2899
AC	0.0014	1	0.0014	66.75	0.0038
BC	0.0000	1	0.0000	0.8934	0.4143
A^2	0.0003	1	0.0003	12.50	0.0385
B^2	0.0004	1	0.0004	17.78	0.0244
C^2	0.0000	1	0.0000	0.4931	0.5331
residual	0.0001	3	0.0000		
total cor	0.0028	12			
std. dev.	0.0046		R^2		0.9774
mean	0.9495		adjusted R^2		0.9094
CV %	0.4847		adeq. precision		12.8331

https://doi.org/10.1021/acsomega.2c03734
ACS Omega 2022, 7, 41968−41980

12.83, which is greater than 4. This shows an adequate signal implying that the model can be used to navigate the design space. Furthermore, the high R^2 implies that the model can only explain 97.74% of the total variation data. The adjusted R^2 value of 90.94% shows a high significance between the predicted and actual values.

The quadratic model derived from the regression analysis of the experimental data is given below:

$$\mathrm{SAC} = 0.9653 + 0.0071A + 0.0059B + 0.0029C + 0.0030AB - 0.0188AC - 0.0022BC - 0.0108A^2 - 0.0128B^2 - 0.0021C^2 \quad (1)$$

where A, B, and C are cellulose, silica, and ZnO (wt %).

Equation 1 shows that the SAC value is directly proportional to the increase in the concentration of cellulose (A), silica (B), ZnO (C), and cellulose−silica interaction (AB), corresponding to a positive constant value. Meanwhile, the interaction between cellulose−ZnO (AC) and silica−ZnO (BC) gave a negative effect on the SAC value.

Figure 1 shows the predicted vs actual values for SAC. The data distribution is relatively close to the straight line,

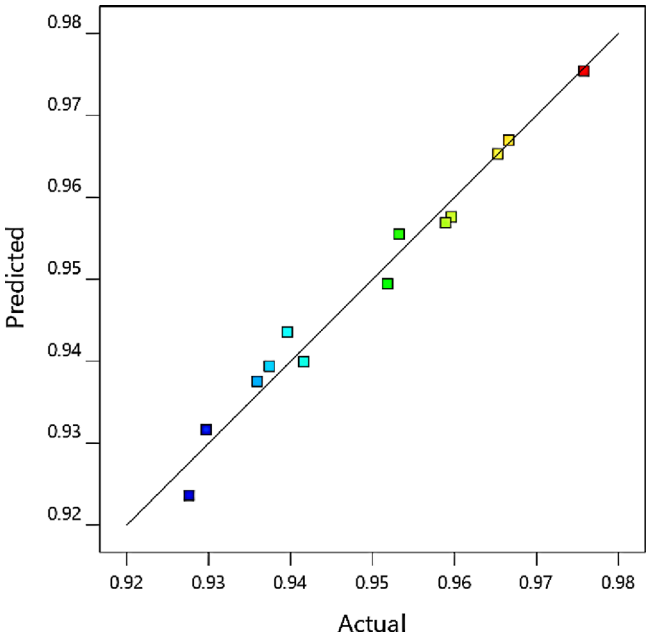

Figure 1. The plot of predicted vs actual value for SAC.

indicating that the regression model can predict the SAC value of cellulose−silica aerogels.

Figure 2a−f shows the variable interaction of the 3D surface and contour plots on SAC response. The orange−red compositions are desirable, while the green−blue compositions are less desirable. In Figure 2a, the optimum results were obtained by adding 35 wt % cellulose and 15 wt % silica. This combination produces a high level of SAC due to the acoustic energy mostly absorbed by the interface between the cellulose fiber and the silica particles.[76] However, adding cellulose and silica content above the optimum point causes a decrease in the SAC value.

In Figure 2c, the reduction in SAC is due to the decreasing cellulose and increasing ZnO concentration. This phenomenon is similar to the results of the studies conducted by Kamal Mohamed et al.[63] that stated that adding ZnO increased cellulose solubility and molecules, resulting in a denser mesh-like surface structure. Since it is difficult for sound waves to pass through larger pores in cellulose, less sound is absorbed. Figure 2e shows that increasing silica and decreasing ZnO concentration improve the SAC value. This phenomenon is related to a smaller silica particle size and more uniform distribution, improving acoustic insulation performance.[76]

The numerical optimization used the desirability function to get the maximum SAC value. Therefore, the optimization aimed to select the cellulose, silica, and ZnO concentration in range and maximize the SAC value. Figure 3 shows the chosen solution formula with the highest desirability level of 1.000, 39.8578 wt % cellulose, 16.5428 wt % silica, 0.5684 wt % ZnO, with an SAC value of 0.9758. After the validation procedure, the measured SAC for the solution formula was 0.9709, with a percentage difference of 0.5%, indicating an outstanding model precision.

Figure 4 shows the SAC value of the cellulose aerogel and cellulose−silica aerogel at different frequencies (50−6400 Hz). The SAC value is directly proportional to the increase in frequency. However, the increase in the sound absorption coefficient was dominant between 2500 and 5000 Hz. Additionally, the cellulose aerogel and cellulose−silica aerogel had the highest SAC values of 0.59 and 0.70 at approximately 4200 and 5000 Hz, respectively. This proves that the incorporation of silica into the cellulose aerogels increased the SAC value, indicating better sound absorption.

X-ray Diffraction (XRD) Analysis. Figure 5 shows the XRD pattern of leached silica, cellulose aerogel, and cellulose−silica aerogel. The round peak appeared at around $2\theta = 22.40°$ for the amorphous silica.[35,77] Meanwhile, the sharp crystalline peaks appeared at 2θ = 12.30, 20.00, and 21.40° for the cellulose aerogel.[78,79] Furthermore, these peaks became weaker and appeared at approximately 2θ = 15−30°, showing that amorphous silica was formed, and the crystalline structure of the cellulose aerogel was significantly destroyed.[80] The explanation for this behavior is probably related to the disruption mechanism, in which the silica particles' in situ composite on the cellulose surfaces disrupts the bundling of fiber into ribbons.[81] These results further show the successful synthesis of cellulose−silica aerogel using waste newspaper and geothermal silica as raw materials by the ambient pressure drying.

Fourier Transform Infrared (FTIR) Spectroscopy. Figure 6 shows the FTIR spectra of leached silica, cellulose aerogel, and cellulose−silica aerogel, while Table 3 summarizes all the FTIR results, which are consistent with previous studies.[67,68,82−84] For leached silica, there was no transmittance peak identified between 2800 and 3000 cm^{-1}, showing that it is purely used and free from organic matter.[85] Furthermore, the peaks for the cellulose−silica aerogel at 3336 and 1156 cm^{-1} were related to the overlapping effect between silica and cellulose.[68] The band at 3336 and 1156 cm^{-1} corresponds to the O−H stretching vibration and Si−O−Si asymmetric stretching vibration, respectively. The results show that silica was impregnated into the cellulose aerogel.

Porous Structure Analysis. Figure 7 shows nitrogen adsorption−desorption isotherms of cellulose aerogel and cellulose−silica aerogel. Type IV isotherms characterize the entire sample, typical of mesoporous materials in the range of 2−50 nm, and are similar to the previous study.[68]Table 4 shows that cellulose aerogel and cellulose−silica aerogel have a surface area of 0.60 and 5.63 m^2/g, respectively. The greater

https://doi.org/10.1021/acsomega.2c03734
ACS Omega 2022, 7, 41968−41980

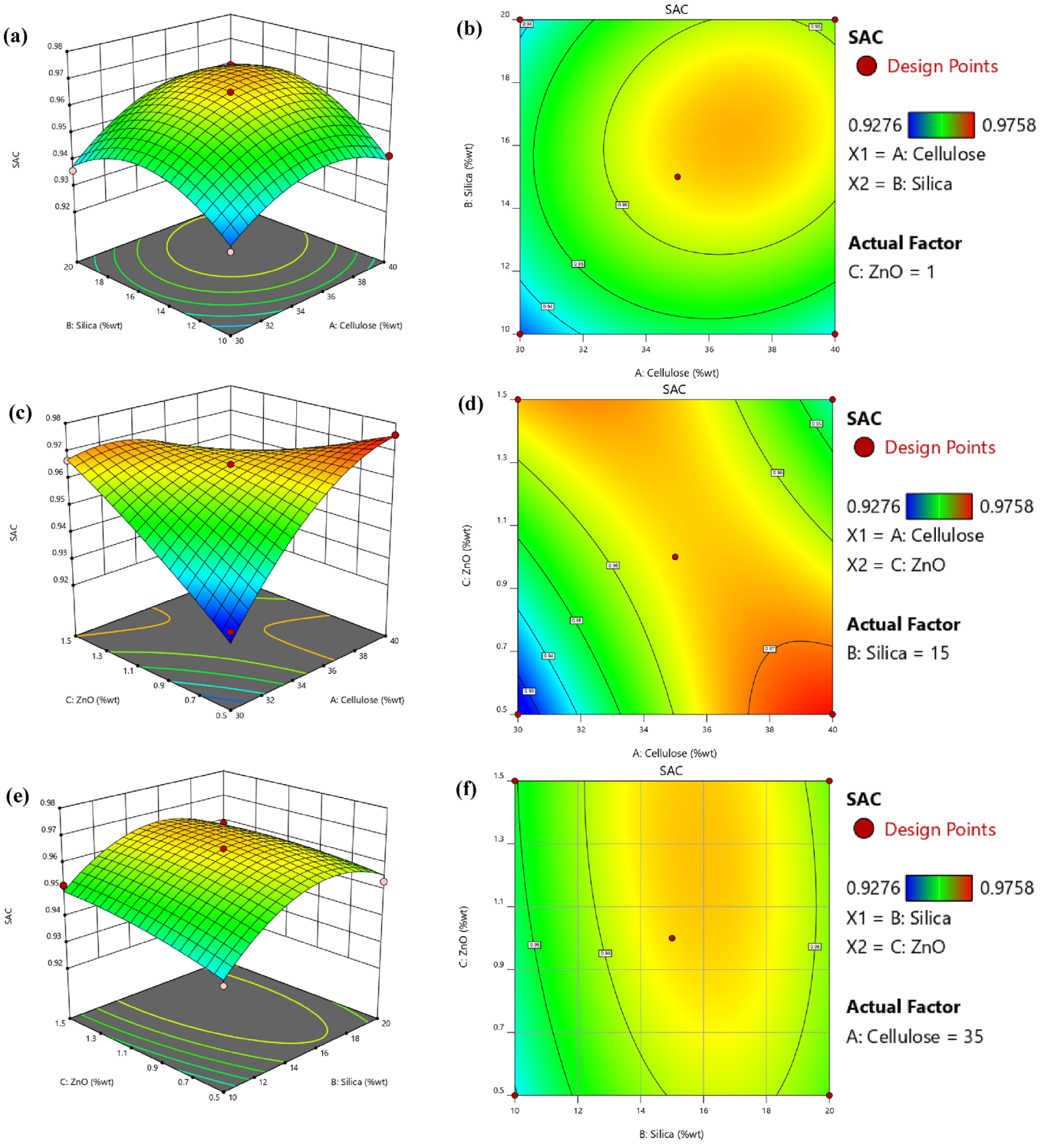

Figure 2. Surface and contour plot of SAC: (a, b) plot of cellulose (A) and silica (B); (c, d) plot of cellulose (A) and ZnO (C); and (e, f) plot of silica (B) and ZnO (C).

surface area of cellulose−silica is due to the silica particles attached to the cellulose fibers, preventing them from shrinking during the regeneration process.[68] However, the surface area of cellulose−silica aerogel is less than that in the study conducted by Demilecamps et al. (220 m^2/g)[66] due to the collapse of the pores during the process of ambient pressure drying.[86] Furthermore, the pore size of the cellulose aerogel was 34.19 nm, and that of the cellulose−silica aerogel decreased by 22.00 nm due to the highest silica attached to the fiber surface. In this study, silica was combined with water to become "swollen", and its particles filled the pore of cellulose and functioned as an "adhesive", resulting in a decrease in pore size.[87]

Scanning Electron Microscope−Energy Dispersive X-ray (SEM−EDX) Analysis. Figure 8 shows the SEM images of cellulose aerogel and cellulose−silica aerogel with significantly different morphologies. Figure 8a shows long cellulose fibers with a rough surface and relatively large pores, as listed in

https://doi.org/10.1021/acsomega.2c03734
ACS Omega 2022, 7, 41968−41980

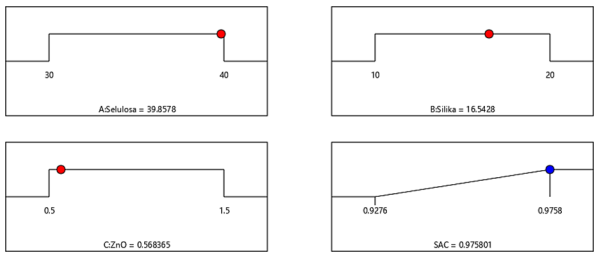

Figure 3. Optimization response of SAC.

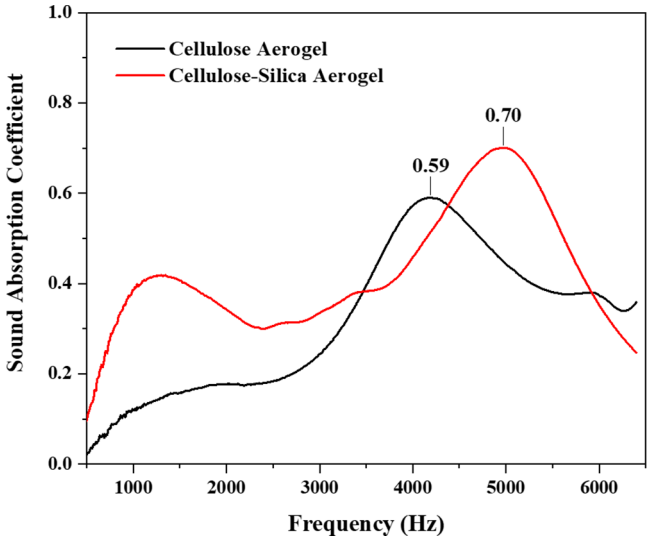

Figure 4. The SAC values of the cellulose aerogel and cellulose−silica aerogel using an impedance tube.

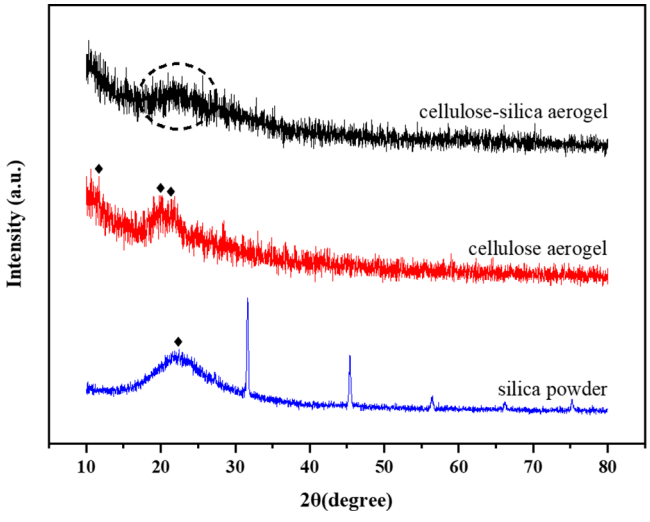

Figure 5. XRD pattern of leached silica, cellulose aerogel, and cellulose−silica aerogel.

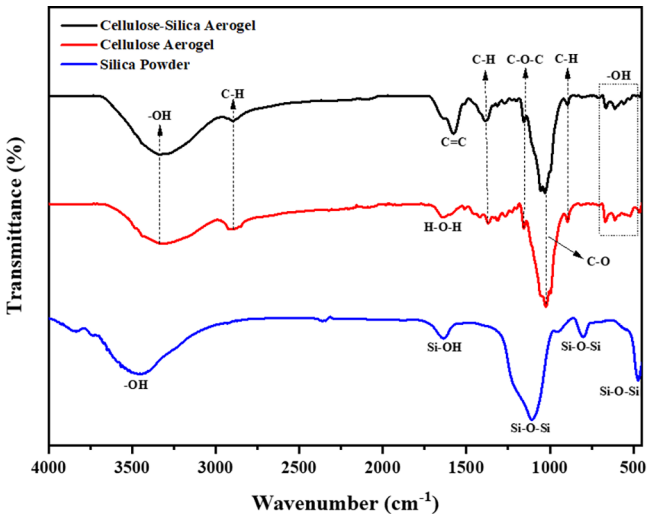

Figure 6. FTIR spectra of leached silica, cellulose aerogel, and cellulose−silica aerogel.

Table 3. FTIR Results for Leached Silica, Cellulose Aerogel, and Cellulose−Silica Aerogel

	wavenumber (cm^{-1})		
assignment	leached silica	cellulose aerogel	cellulose−silica aerogel
O−H stretching vibration	3446		
silanol stretching vibration	1638		
Si−O−Si asymmetric stretching vibration	1107		
Si−O−Si symmetric stretching vibration	800		
Si−O−Si bending vibration	471		
O−H stretching vibration		3331	
C−H stretching vibration		2892	
H−O−H bending vibration of absorbed water		1640	
C−H deformation vibration		1367	
C−O−C asymmetric stretching vibration		1156	
C−O symmetric stretching of primary ethanol		1024	
C−H bending vibration		894	
O−H bending vibration		450−670	
O−H stretching vibration			3336
C−H stretching vibration			2901
C═C stretching vibration			1576
C−H deformation vibration			1389
Si−O−Si asymmetric stretching vibration			1156
C−O symmetric stretching of primary ethanol			1029
C−H bending vibration			895
O−H bending vibration			450−670

Table 4. In contrast, Figure 8b shows silica particles attached and evenly distributed to the surface of the fibers. During the regeneration process, the silanols in the silica sol combine with the cellulose molecules through the dehydrating action between the hydroxyl groups.[68] Conclusively, the silanols covering the surface of cellulose fibers continue to condense, which result in complex structures. In addition, the hydrogen bonding among cellulose, silica, and solvent enhanced the homogeneous network structure;[87] hence, the silica forms finer cellulose fibers.[67]

Figure 9 shows the elemental composition analysis of the cellulose aerogel and cellulose−silica aerogel. The cellulose aerogel contains C, O, Na, Ca, and Zn elements, while the cellulose−silica aerogel contains C, O, Na, Al, Si, Cl, K, Ca, and Zn elements. Furthermore, EDX confirmed the presence of silicon inside the cellulose−silica aerogel, while other elements are probably derived from geothermal silica. The

https://doi.org/10.1021/acsomega.2c03734
ACS Omega 2022, 7, 41968−41980

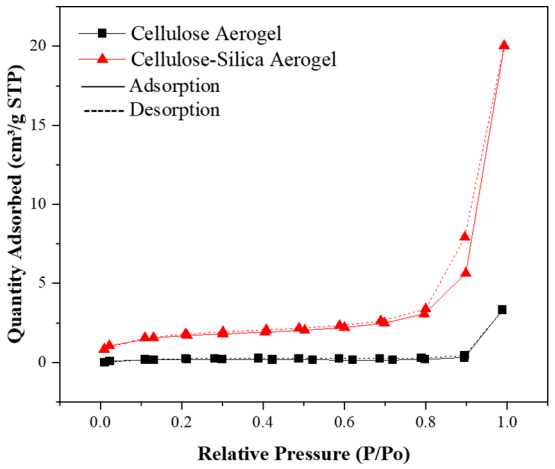

Figure 7. The nitrogen adsorption−desorption isotherms of cellulose aerogel and cellulose−silica aerogel.

Table 4. Physical Properties of Cellulose Aerogel and Cellulose−Silica Aerogel

sample	surface area (m^2/g)	pore volume (cm^3/g)	pore size (nm)
cellulose aerogel	0.60	0.01	34.19
cellulose−silica aerogel	5.63	0.03	22.00

signal for the silicon atoms and the carbon and oxygen peaks from the cellulose network is identified at 1.74, 0.28, and 0.53 keV, respectively. This result is similar to a previous study.[36] Meanwhile, the EDX analysis is only used to verify the presence of silicon atoms and not to quantify their amount and location.[88]

Thermal Gravimetric Analysis (TGA). Figures 10 and 11 show the cellulose aerogel's and cellulose−silica aerogel's TG/DTG curves, respectively. The thermal decomposition of cellulose aerogel consists of three phases, namely, 25−105 °C with 10.38%, 106−370 °C with 60.26%, and 371−900 °C with 10.66% weight loss. The evaporation of adsorbed water and some organic components occurs in the first,[67,68] while the second and third stages are associated with the degradation and decomposition of cellulose and some organic components.[68,81] Therefore, the mass of most cellulose aerogel is lost at this stage. Furthermore, when heated to a higher degree, the cellulose aerogel loses its structural stability, resulting in a total collapse.[35]

The thermal decomposition of cellulose−silica aerogel consists of four phases, namely, 25−105 °C with 12.77%, 106−350 °C with 39.89%, 351−500 °C with 8.57%, and 501−900 °C with 5.57% weight loss. At temperatures above 500 °C, the residual ash generally consists of silica. The cellulose−silica aerogel has a smaller mass loss compared to the cellulose aerogel. This is due to the increase of silica and the decrease of cellulose content in composite aerogels, which cause the weakening of their synergistic effect and also the transformation of the framework structure from cellulose to silica-dominated.[67] However, the curves showed that the cellulose−silica aerogel has a significant weight loss at 300−400 °C with the presence of ZnO, where lignocellulose was highly sensitive to inorganic salts as reported in a previous study.[89] At 900 °C, the weight loss of cellulose−silica aerogel was 66.80%, indicating that silica can significantly stabilize the cellulose against decomposition.[36]

Table 5 shows the previous studies on SAC from the material-based aerogel. Although the cellulose−silica aerogel was made from recycle cellulose fiber and geothermal silica, it has a high SAC value compared to several previous studies. Sadly, this value is lower than that in the research conducted by Silviana et al.[73] This is probably due to the use of different chemicals to improve the solubility of NaOH solution. The previous study used polyethylene glycol (PEG), which can stabilize cellulose solution.[62] However, ZnO has the ability to form stronger hydrogen bonds with cellulose, which improve the solubility of cellulose.[63] The addition of ZnO to the NaOH/water solution leads to the production of smaller particles and a hydroxide layer (≡Zn−OH) on the particle surface. These hydroxide species readily bind to water and reduce the volume of water molecules close to the cellulose chain, hence inhibiting aggregation and delaying gelation.[94] Furthermore, the cellulose−silica aerogel belongs to sound absorption class A (ISO 11654), which is the best sound absorption category.

CONCLUSIONS

This study successfully synthesized cellulose−silica aerogel using waste newspaper-based cellulose, geothermal silica, and NaOH/ZnO solution with ambient pressure drying. The result

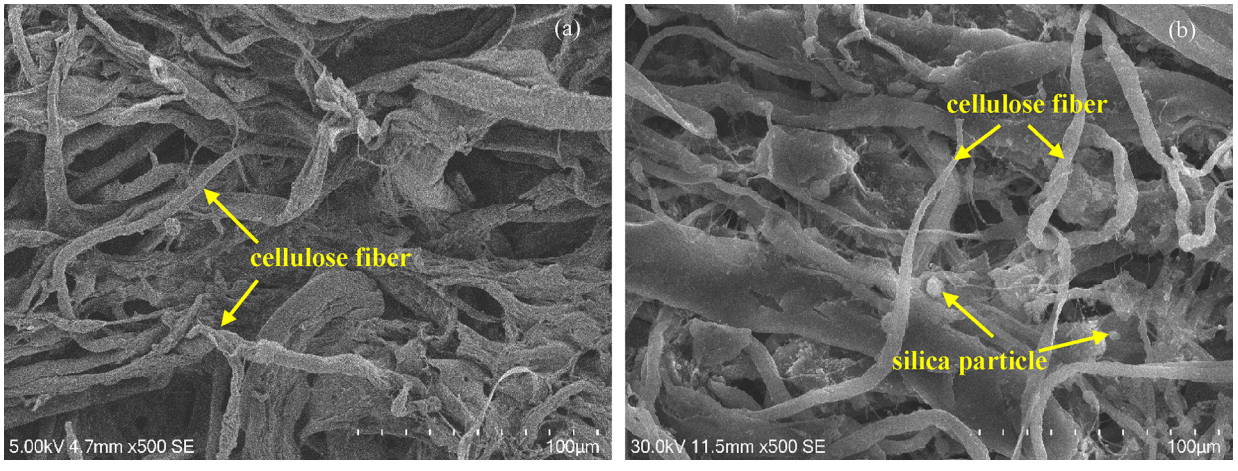

Figure 8. SEM image of (a) cellulose aerogel and (b) cellulose−silica aerogel.

https://doi.org/10.1021/acsomega.2c03734
ACS Omega 2022, 7, 41968−41980

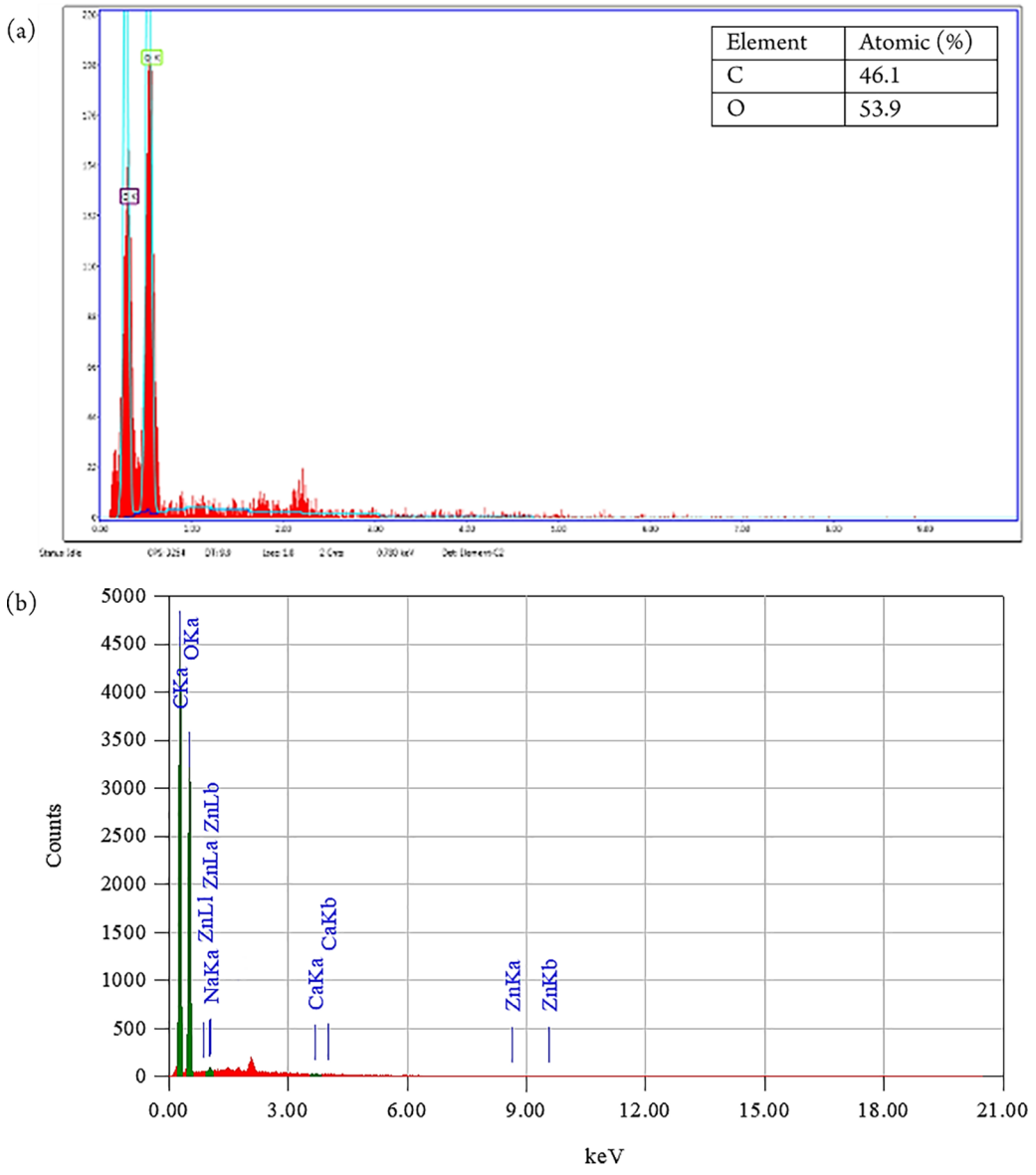

Figure 9. EDX mapping of (a) cellulose aerogel and (b) cellulose−silica aerogel.

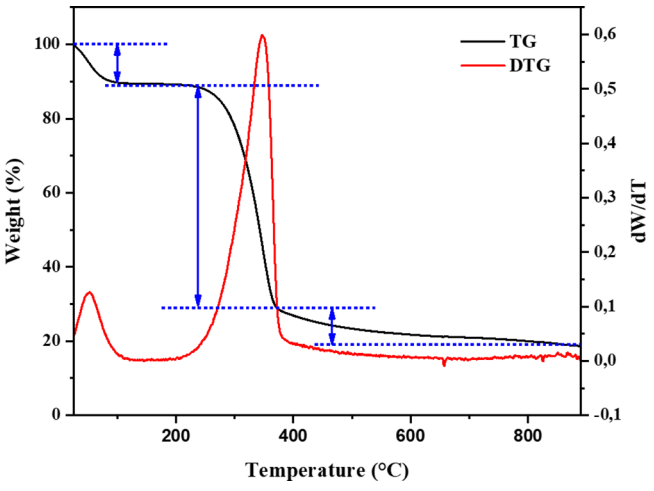

Figure 10. TG/DTG curves of cellulose aerogel.

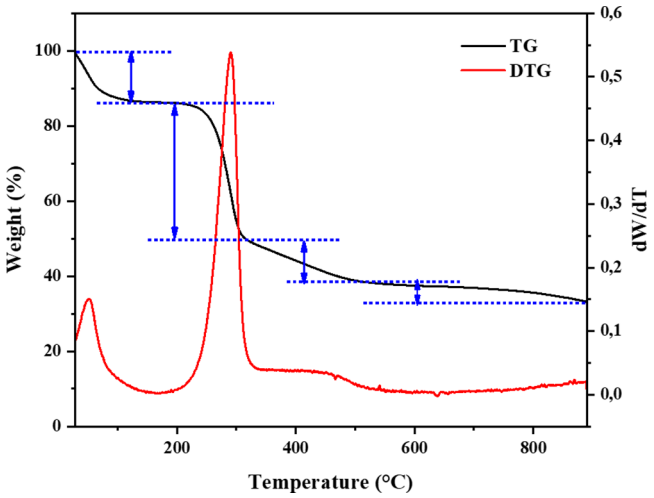

Figure 11. TG/DTG curves of cellulose−silica aerogel.

https://doi.org/10.1021/acsomega.2c03734
ACS Omega 2022, 7, 41968−41980

Table 5. Comparison of SAC Value with Other Studies

material	method	t (cm)	frequency (Hz)	SAC	author
MTMS-VTMS derived aerogel	impedance tube	1.6	200−2500	0.9	Cai et al.[90]
polyimide-silica aerogel	impedance tube	1 and 3	2500−10,000	0.8	Yan et al.[91]
silica aerogel, GSA-SDS aerogel	impedance tube (Brüel & Kjær)	1−5	50−1600	0.86	Sachithanadam and Joshi[92]
cellulose−silica aerogel	impedance tube (Brüel & Kjær)	1	50−6400	0.70	this study
monolithic silica aerogel	impedance tube (Brüel & Kjær)	1.27−2.54	100−4900	0.88	Merli et al.[93]
silica−cellulose aerogel	sound level meter	1	31.5−8000	0.39−0.50	Feng et al.[35]
silica−cellulose aerogel	sound level meter	1	31.5−8000	0.9896	Silviana et al.[73]
cellulose−silica aerogel	sound level meter	1	31.5−8000	0.9709	this study

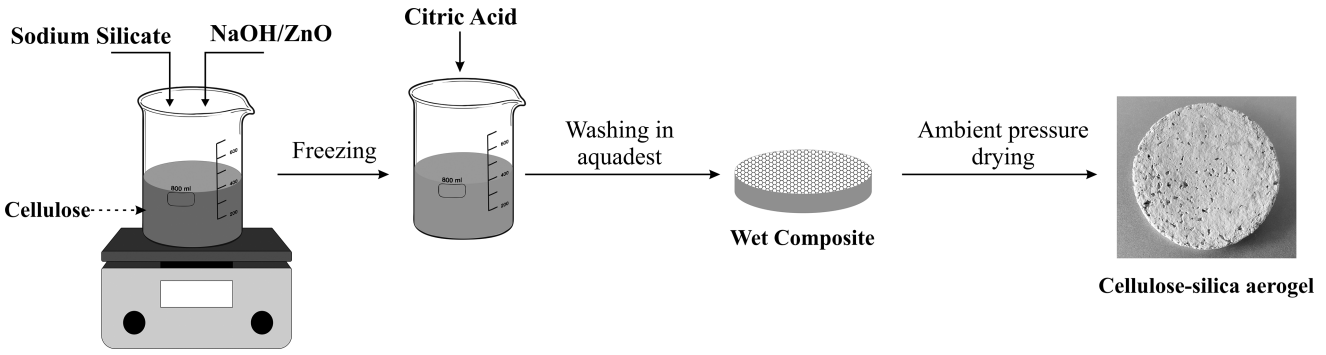

Figure 12. Scheme of cellulose−silica aerogel preparation.

shows that the silica impregnated cellulose aerogel is a better sound-insulating material. Furthermore, the distribution of this compound on the surface of cellulose enhances the network structure due to the hydrogen bond among cellulose, silica, and solvent. Its presence increases the surface area but decreases the pore size of cellulose−silica aerogel. Silica also contributes to improving the thermal stability of cellulose−silica aerogel. Additionally, the optimum SAC was obtained at 39.8578 wt % cellulose, 16.5428 wt % silica, 0.5684 wt % ZnO. The results of ANOVA show a significant model with p value, R^2, and adj R^2 of 0.0252, 97.74%, and 90.94%, respectively. These results are essential for the future development of cellulose−silica aerogels, especially for the improvement of drying methods.

MATERIALS AND METHODS

Materials. The waste newspaper was collected locally in Semarang, and geothermal silica was supplied from PT Geo Dipa Energi, Dieng, Indonesia. Furthermore, zinc oxide (ZnO) powder was purchased from SmartLab in the same country. Sulfuric acid (H_2SO_4, purity 98%), sodium hydroxide (NaOH, purity 98%), and citric acid ($C_6H_8O_7$, purity 98%) were purchased from Merck, Germany, and used without further purification. Finally, the preparation was performed using distilled water.

Methods. *Pretreatment of Geothermal Silica.* Pretreatment was performed to remove organic and residual impurities in geothermal silica based on the procedures in previous studies but with some modifications.[95,96] Geothermal silica was dried at 105 °C for 24 h and mixed with sulfuric acid at 90 °C for 3 h, and the ratio of silica to H_2SO_4 was 1:5 (w/v). After the slurry was formed, the solution was screened through a filter paper, washed until the neutral pH was reached, and then dried at 110 °C until it achieved a constant weight. Afterward, the silica was soaked in a 2 N sodium hydroxide solution and dried for 1 h at 95 °C. Subsequently, the solution was screened through a filter paper to separate sodium silicate (Na_2SiO_3) and the solid residue.

Preparation of Cellulose from Waste Newspaper. The waste newspaper was treated by chemical extraction to remove ink and glue based on the procedures in the previous studies.[17,18] It was cut into small pieces (1−2 cm), soaked in a 2 N sodium hydroxide solution, heated at 80 °C, and stirred for 3 h. Afterward, it was left overnight at ambient temperature. The mixture was then screened and washed with distilled water at least five times until a neutral pH was obtained.

Preparation of Cellulose Aerogel. The method used for the cellulose aerogel preparation is based on the procedures in the previous studies with some modifications.[62] Cellulose and NaOH/ZnO aqueous solution were stirred for 1 h, frozen for 12 h at −15 °C, and then thawed at ambient temperature with constant stirring for 30 min. The cake was immersed in 0.2 M citric acid to neutralize sodium hydroxide after being frozen at −15 °C for a further 12 h. The solution was filtered and washed with distilled water until it reached a neutral pH. Subsequently, it was dried in an oven at 90, 100, and 110 °C for 90 min each.

Preparation of Cellulose−Silica Aerogel. The preparation of cellulose−silica aerogel as shown in Figure 12 is based on the procedures in the previous studies with some modifications.[62,66] First, cellulose, Na_2SiO_3, and NaOH/ZnO aqueous solution were stirred for 1 h. Furthermore, the solutions were frozen for 12 h at −15 °C and then thawed at ambient temperature with constant stirring for 30 min. The cake was immersed in 0.2 M citric acid to neutralize sodium hydroxide after being frozen at −15 °C for a further 12 h. The solution was filtered and washed with distilled water until it reached a neutral pH. It was then dried in an oven at 90, 100, and 110 °C for 90 min in each.

Design Experiment. The Box−Behnken design using the Design-Expert software (version 12.0) was used to determine the effect of cellulose, silica, and ZnO concentrations on SAC value. Table 6 shows the coded levels for these variables. The

https://doi.org/10.1021/acsomega.2c03734
ACS Omega 2022, 7, 41968−41980

Table 6. Coded Level BBD

variable	symbol	coded level		
		−1	0	1
cellulose (wt %)	x_1	30	35	40
silica (wt %)	x_2	10	15	20
ZnO (wt %)	x_3	0.5	1	1.5

ZnO variable was based on the previous study of Demilecamps et al.[66] using an upper and lower range approach. However, the cellulose, silica, and ZnO were mixed with varying concentrations and dried for different periods in a preliminary study.

Measurement of Sound Absorption Coefficient. The methods used to measure the SAC of cellulose−silica aerogel in this study are a sound level meter and an impedance tube.

Study of the Sound Level Meter. This method was conducted according to a previous study.[35] Figure 13 shows

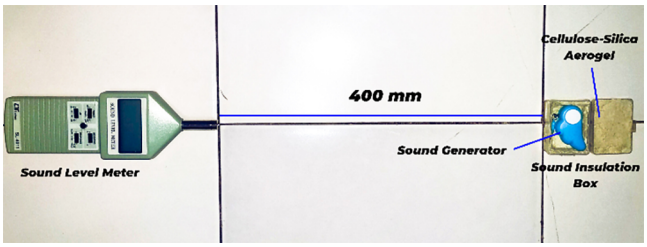

Figure 13. Measurement of SAC using the sound level meter.

that the sound absorption coefficient of the cellulose−silica aerogels with a thickness of 10 mm was studied using a sound level meter (Lutron SL-4011) and a sound signal generator (Blesi Guardian Angel self-protection alarm, 90 dB). The sound generator was housed inside an insulation box made by fixing cellulose−silica aerogels at all sides to ensure a closed system. Furthermore, the incident sound signal was measured 400 mm away from the generator source.

The following equation is used to calculate the sound absorption coefficient measured by the sound level meter:

$$\mathrm{Li} = 10\log_{10}\left(\frac{I}{I_0}\right)\mathrm{dB} \tag{2}$$

where Li, I, and I_0 are the sound intensity level (dB), the sound intensity (W/m^2), and the reference sound intensity (10^{-12} W/m^2).

The sound absorption coefficient (SAC) is the fraction of sound energy absorbed by the material. It represents a value in the range of 0 to 1. It can be expressed as:

$$\alpha = 1 - \frac{I_R}{I_I} \tag{3}$$

where α, I_R, and I_I are the sound absorption coefficient, the reflected sound intensity, and the incident sound intensity.

Study of the Impedance Tube. An impedance tube compared the sound absorption coefficient measured using the sound level meter (the theoretically calculated value). This is because it is a compact setup that can easily and affordably determine small samples' absorption data.[97] Furthermore, the optimum SAC value was used to measure cellulose−silica aerogel and cellulose aerogel (silica free) with a 3 cm diameter and a 1 cm thickness. Figure 14 shows that the Brüel & Kjær Impedance Tube Kit Type 4206 measured the sound

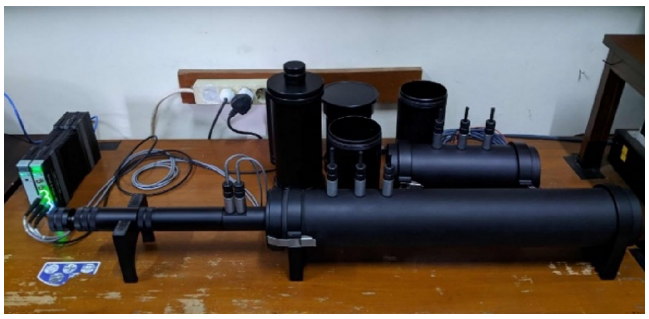

Figure 14. Measurement of SAC using the impedance tube.

absorption coefficient at a frequency in the range of 50 Hz to 6.4 kHz. Additionally, the absorption coefficient measurements using the two-microphone transfer-function method were according to ISO 10534-2 and ASTM E1050-12 international standards. The measurements were made with two $^1/_4$ in. Condenser Microphones Type 4187, fitted with Type 4206, specially designed to reduce errors due to pressure leakage at high frequencies. Meanwhile, the sound absorption coefficient was calculated from the sound pressures in the incident and reflected wave.

Characterization. The structures of the aerogels were analyzed using an X-Ray diffractometer (XRD, PANalytical X'Pert PRO). The patterns of XRD were recorded in the 2θ range of 10 to 90°. Furthermore, their functional groups were identified using an FTIR spectrophotometer (Perkin-Elmer UATR Two) with the ATR method. The IR spectra were recorded from 4000 to 450 cm^{-1}. The morphology of aerogels was investigated using a scanning electron microscope (SEM, Jeol JSM-IT200) at an acceleration voltage (VACC) of 5 kV. Also, the distribution and elemental composition of silica particles were determined using an energy-dispersive X-ray (EDX) spectrometer, which was coupled with the SEM. The nitrogen gas sorption/physisorption was measured at −195.85 °C using Micromeritics TriSar II 3020 Version 2.00. Additionally, the surface area of aerogels and the pore size distributions were determined using Brunauer−Emmett−Teller (BET) and Barrett−Joyner−Halenda (BJH) methods, respectively. Finally, their thermal stability was analyzed using thermogravimetric analysis (TG) with the simultaneous thermogravimetric analyzer NEXTA STA (Hitachi STA200RV with real view sample observation). The samples were heated in flowing air from ambient temperature to 900 °C at 10 °C min^{-1}.

■ ECONOMIC ANALYSIS OF AEROGEL PRODUCTION

The economic analysis of aerogel production should be as detailed as possible, with all the important elements included. This study is focused on the material and energy costs, which are the most crucial parameters to consider. Table 7 shows the material costs that we used. Since the cellulose fiber was extracted from waste newspaper and silica from geothermal solid waste, these materials are available free of charge. However, transportation costs for silica are $40, and transportation costs for other materials are the responsibility of the company that supplies raw materials for aerogel manufacturing.

The following equation expresses the energy costs required to manufacture 1 kg of aerogel:

https://doi.org/10.1021/acsomega.2c03734
ACS Omega 2022, 7, 41968−41980

Table 7. Material Costs for the Synthesis of Cellulose−Silica Aerogel

material	cost ($/kg of aerogel)
ZnO	0.8
H_2SO_4 (98%)	50
NaOH (98%)	40
$C_6H_8O_7$ (0.2 M)	60
distilled H_2O	0.9

$$C_e = T \times n_h \times P \quad (4)$$

where C_e, T, n_h, and P are the energy cost ($/kg of aerogel), 1 kWh of electricity cost ($/kWh), number of operating hours (h), and power (W). The energy costs are calculated according to eq 4, as shown in Table 8.

Table 8. Energy Costs for the Synthesis of Cellulose−Silica Aerogel

process	energy cost ($/kg of aerogel)
stirring	0.01
freezing	0.24
drying	0.56

Garrido et al.[98] studied the manufacture of inorganic aerogel (IA) and two hybrid aerogels produced in powder (HYB-A) and monolithic (HYB-C) forms. Table 9 and Figure 15 show

Table 9. Total Cost of the Aerogels

aerogel	cost ($/kg of aerogel)			total costs
	material	energy	transport	
CSA	151.7	0.81	40	192.51
IA	439.83	12.66		588.66
HYB-A	645.03	3.19		648.22
HYB-C	722.03	12.66		734.69

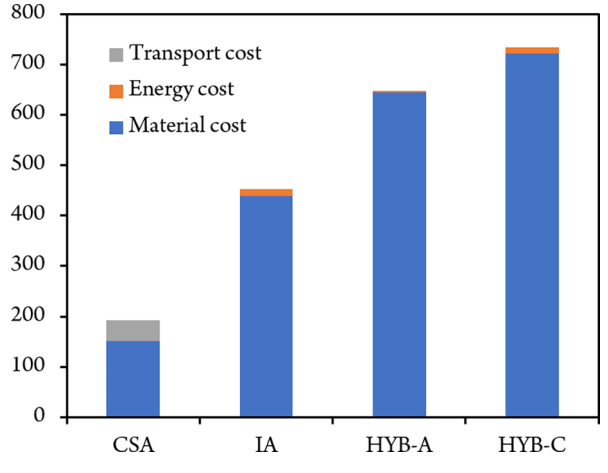

Figure 15. Total cost for aerogel production.

an overview of the total material cost for several types of aerogels. When compared to the silica-based aerogels, cellulose−silica aerogel (CSA) is the cheapest acoustic insulating material despite the fact that there is a $40 transportation cost. It is obvious that the utilization of recycled materials reduces the production cost of cellulose−silica aerogel and can be scaled up for industrial applications.

AUTHOR INFORMATION

Corresponding Author

S. Silviana − *Department of Chemical Engineering, Faculty of Engineering, Diponegoro University, Semarang 50275, Indonesia*; orcid.org/0000-0002-8831-0147; Email: silviana@che.undip.ac.id

Authors

Enggar C. Prastiti − *Department of Chemical Engineering, Faculty of Engineering, Diponegoro University, Semarang 50275, Indonesia*

Ferry Hermawan − *Department of Civil Engineering, Faculty of Engineering, Diponegoro University, Semarang 50275, Indonesia*

Agus Setyawan − *Department of Physics, Faculty of Science and Mathematics, Diponegoro University, Semarang 50275, Indonesia*

Complete contact information is available at: https://pubs.acs.org/10.1021/acsomega.2c03734

Notes

The authors declare no competing financial interest.

ACKNOWLEDGMENTS

The authors are thankful to the AMaL (Advanced Material Laboratory) community of Diponegoro University for their support and discussion throughout the research. This research was financially supported by the Directorate of Research, Technology, and Community Service, Directorate General of Higher Education, Research, and Technology, Ministry of Education, Culture, Research, and Technology, of the Republic of Indonesia through Master Thesis Research grant SP DIPA-023.17.1.690523/2022 under Implementation Agreement 345-69/UN7.6.1/PP/2022.

ABBREVIATIONS

ZnO, zinc oxide; NaOH, sodium hydroxide; BBD, Box−Behnken design; SAC, sound absorption coefficient; XRD, X-ray diffraction; FTIR, Fourier-transform infrared; SEM−EDX, scanning electron microscopy−energy-dispersive X-ray; BET−BJH, Brunauer, Emmett, Teller−Barrett, Joyner, Halenda; TGA, thermal gravimetric analysis

REFERENCES

(1) Münzel, T.; Schmidt, F. P.; Steven, S.; Herzog, J.; Daiber, A.; Sørensen, M. Environmental Noise and the Cardiovascular System. *J. Am. Coll. Cardiol.* **2018**, *71*, 688−697.

(2) Kim, K.; Shin, J.; Oh, M.; Jung, J. K. Economic Value of Traffic Noise Reduction Depending on Residents' Annoyance Level. *Environ. Sci. Pollut. Res.* **2019**, *26*, 7243−7255.

(3) Schmidt, F. P.; Basner, M.; Kröger, G.; Weck, S.; Schnorbus, B.; Muttray, A.; Sariyar, M.; Binder, H.; Gori, T.; Warnholtz, A.; Münzel, T. Effect of Nighttime Aircraft Noise Exposure on Endothelial Function and Stress Hormone Release in Healthy Adults. *Eur. Heart J* **2013**, *34*, 3508.

(4) Kwon, N.; Park, M.; Lee, H.-S.; Ahn, J.; Shin, M. Construction Noise Management Using Active Noise Control Techniques. *J. Constr. Div., Am. Soc. Civ. Eng.* **2016**, *142*, No. 04016014.

(5) Peng, L.*Sound Absorption and Insulation Functional Composites*; Elsevier Ltd, 2017, DOI: 10.1016/B978-0-08-100411-1.00013-3.

(6) Yang, Y.; Li, B.; Chen, Z.; Sui, N.; Chen, Z.; Xu, T.; Li, Y.; Fu, R.; Jing, Y. Sound Insulation of Multi-Layer Glass-Fiber Felts: Role of Morphology. *Text. Res. J.* **2017**, *87*, 261−269.

(7) Bai, P.; Yang, X.; Shen, X.; Zhang, X.; Zhu, J.; Yin, Q.; Li, Z.; Wang, C.; Xu, L. Investigation on Sound Absorbing Performance of the Polyester Fiber for Noise Reduction in Large-Scale Equipment. *IOP Conf. Ser.: Mater. Sci. Eng.* **2018**, *398*, No. 012004.
(8) López, J. P.; El Mansouri, N. E.; Alba, J.; Del Rey, R.; Mutjé, P.; Vilaseca, F. Acoustic Properties of Polypropylene Composites Reinforced with Stone Groundwood. *BioResources* **2012**, *7*, 4586−4599.
(9) Yu, T.; Jiang, F.; Wang, J.; Wang, Z.; Chang, Y.; Guo, C. Acoustic Insulation and Absorption Mechanism of Metallic Hollow Spheres Composites with Different Polymer Matrix. *Compos. Struct.* **2020**, *248*, No. 112566.
(10) Ji, Y.; Chen, S.; Cheng, Y. Synthesis and Acoustic Study of a New Tung Oil-Based Polyurethane Composite Foam with the Addition of Miscanthus Lutarioriparius. *Polymers* **2019**, *11*, 1144.
(11) Yang, Y.; Chen, Z.; Xu, T.; Han, R.; Emefa Awuye, D. Sound Insulation and Hydrophobic Properties of Phenolic Resin Modified Melamine Foam: Role of Micro-Morphology. *Mater. Res. Express* **2019**, *6*, No. 075331.
(12) Zhang, C.; Gong, J.; Li, H.; Zhang, J. Fiber-Based Flexible Composite with Dual-Gradient Structure for Sound Insulation. *Composites, Part B* **2020**, *198*, No. 108166.
(13) Arenas, J. P.; del Rey, R.; Alba, J.; Oltra, R. Sound-Absorption Properties of Materials Made of Esparto Grass Fibers. *Sustainability* **2020**, *12*, 5533.
(14) Zhu, X.; Kim, B. J.; Wang, Q. W.; Wu, Q. Recent Advances in the Sound Insulation Properties of Bio-Based Materials. *BioResources* **2013**, *9*, 1−23.
(15) Fu, B.; Yang, Q.; Yang, F. Flexible Underwater Oleophobic Cellulose Aerogels for Efficient Oil/Water Separation. *ACS Omega* **2020**, *5*, 8181−8187.
(16) Pongchaiphol, S.; Preechakun, T.; Raita, M.; Champreda, V.; Laosiripojana, N. Characterization of Cellulose-Chitosan-Based Materials from Different Lignocellulosic Residues Prepared by the Ethanosolv Process and Bleaching Treatment with Hydrogen Peroxide. *ACS Omega* **2021**, *6*, 22791−22802.
(17) Srasri, K.; Thongroj, M.; Chaijiraaree, P.; Thiangtham, S.; Manuspiya, H.; Pisitsak, P.; Ummartyotin, S. Recovery Potential of Cellulose Fiber from Newspaper Waste: An Approach on Magnetic Cellulose Aerogel for Dye Adsorption Material. *Int. J. Biol. Macromol.* **2018**, *119*, 662−668.
(18) Takagi, H.; Nakagaito, A. N.; Bistamam, M. S. A. Extraction of Cellulose Nanofiber from Waste Papers and Application to Reinforcement in Biodegradable Composites. *J. Reinf. Plast. Compos.* **2013**, *32*, 1542−1546.
(19) Kadam, A. A.; Lone, S.; Shinde, S.; Yang, J.; Saratale, R. G.; Saratale, G. D.; Sung, J.-S.; Kim, D. Y.; Ghodake, G. Treatment of Hazardous Engineered Nanomaterials by Supermagnetized α-Cellulose Fibers of Renewable Paper-Waste Origin. *ACS Sustainable Chem. Eng.* **2019**, *7*, 5764−5775.
(20) Pandi, N.; Sonawane, S. H.; Anand Kishore, K. Synthesis of Cellulose Nanocrystals (CNCs) from Cotton Using Ultrasound-Assisted Acid Hydrolysis. *Ultrason. Sonochem.* **2021**, *70*, No. 105353.
(21) Ouajai, S.; Shanks, R. A. Preparation, Structure and Mechanical Properties of All-Hemp Cellulose Biocomposites. *Compos. Sci. Technol.* **2009**, *69*, 2119−2126.
(22) Han, Q.; Gao, X.; Zhang, H.; Chen, K.; Peng, L.; Jia, Q. Preparation and Comparative Assessment of Regenerated Cellulose Films from Corn (Zea Mays)Stalk Pulp Fines in DMAc/LiCl Solution. *Carbohydr. Polym.* **2019**, *218*, 315−323.
(23) Lu, P.; Hsieh, Y. L. Preparation and Characterization of Cellulose Nanocrystals from Rice Straw. *Carbohydr. Polym.* **2012**, *87*, 564−573.
(24) Chen, H.; Wang, W.; Martin, J. C.; Oliphant, A. J.; Doerr, P. A.; Xu, J. F.; DeBorn, K. M.; Chen, C.; Sun, L. Extraction of Lignocellulose and Synthesis of Porous Silica Nanoparticles from Rice Husks: A Comprehensive Utilization of Rice Husk Biomass. *ACS Sustainable Chem. Eng.* **2013**, *1*, 254−259.
(25) Rajan, K.; Carrier, D. J. Insights into Exo -Cellulase Inhibition by the Hot Water Hydrolyzates of Rice Straw. *ACS Sustainable Chem. Eng.* **2016**, *4*, 3627−3633.
(26) Hu, S.; Gu, J.; Jiang, F.; Hsieh, Y.-L. Holistic Rice Straw Nanocellulose and Hemicelluloses/Lignin Composite Films. *ACS Sustainable Chem. Eng.* **2016**, *4*, 728−737.
(27) Jin, C.; Han, S.; Li, J.; Sun, Q. Fabrication of Cellulose-Based Aerogels from Waste Newspaper without Any Pretreatment and Their Use for Absorbents. *Carbohydr. Polym.* **2015**, *123*, 150−156.
(28) Fan, P.; Yuan, Y.; Ren, J.; Yuan, B.; He, Q.; Xia, G.; Chen, F.; Song, R. Facile and Green Fabrication of Cellulosed Based Aerogels for Lampblack Filtration from Waste Newspaper. *Carbohydr. Polym.* **2017**, *162*, 108−114.
(29) Asdrubali, F.; Schiavoni, S.; Horoshenkov, K. V. A Review of Sustainable Materials for Acoustic Applications. *Build. Acoust.* **2012**, *19*, 283−311.
(30) Long, L.-Y.; Weng, Y.-X.; Wang, Y.-Z. Cellulose Aerogels: Synthesis, Applications, and Prospects. *Polymers* **2018**, *10*, 623.
(31) Illera, D.; Mesa, J.; Gomez, H.; Maury, H. Cellulose Aerogels for Thermal Insulation in Buildings: Trends and Challenges. *Coatings* **2018**, *8*, 345.
(32) Maleki, H. Recent Advances in Aerogels for Environmental Remediation Applications: A Review. *Chem. Eng. J.* **2016**, *300*, 98−118.
(33) Tripathi, A.; Khan Saad, A.; Rojas, O.; Parsons, G.; Steach, Jeremy. K.; De Witt, Jos. S.; Islam, S.M. B.; Goodrich, Jacob. D.Cellulose-Acetate Aerogels. 2017, p 104.
(34) Nguyen, S. T.; Feng, J.; Ng, S. K.; Wong, J. P. W.; Tan, V. B. C.; Duong, H. M. Advanced Thermal Insulation and Absorption Properties of Recycled Cellulose Aerogels. *Colloids Surf., A* **2014**, *445*, 128−134.
(35) Feng, J.; Le, D.; Nguyen, S. T.; Tan Chin Nien, V.; Jewell, D.; Duong, H. M. Silica-Cellulose Hybrid Aerogels for Thermal and Acoustic Insulation Applications. *Colloids Surf., A* **2016**, *506*, 298−305.
(36) Yuan, B.; Zhang, J.; Mi, Q.; Yu, J.; Song, R.; Zhang, J. Transparent Cellulose−Silica Composite Aerogels with Excellent Flame Retardancy via an in Situ Sol−Gel Process. *ACS Sustainable Chem. Eng.* **2017**, *5*, 11117−11123.
(37) Lu, Y.; Li, X.; Yin, X.; Utomo, H. D.; Tao, N. F.; Huang, H. Silica Aerogel as Super Thermal and Acoustic Insulation Materials. *J. Environ. Prot.* **2018**, *09*, 295−308.
(38) Rudaz, C.; Courson, R.; Bonnet, L.; Calas-Etienne, S.; Sallée, H.; Budtova, T. Aeropectin: Fully Biomass-Based Mechanically Strong and Thermal Superinsulating Aerogel. *Biomacromolecules* **2014**, *15*, 2188−2195.
(39) Cai, J.; Liu, S.; Feng, J.; Kimura, S.; Wada, M.; Kuga, S.; Zhang, L. Cellulose-Silica Nanocomposite Aerogels by in-Situ Formation of Silica in Cellulose Gel. *Angew. Chem.* **2012**, *51*, 2076−2079.
(40) Maury, S.; Buisson, P.; Perrard, A.; Pierre, A. C. Influence of the Sol-Gel Chemistry on the Activity of a Lipase Encapsulated in a Silica Aerogel. *J. Mol. Catal. B: Enzym.* **2004**, *29*, 133−148.
(41) Matias, T.; Marques, J.; Quina, M. J.; Gando-Ferreira, L.; Valente, A. J. M.; Portugal, A.; Durães, L. Silica-Based Aerogels as Adsorbents for Phenol-Derivative Compounds. *Colloids Surf., A* **2015**, *480*, 260−269.
(42) Lei, Y.; Chen, X.; Hu, Z.; Song, H.; Cao, B. A General Strategy for Improving the Thermal Insulation Performance of Aerogels by Multiple Impregnation. *Scr. Mater.* **2017**, *139*, 5−8.
(43) Kim, T. G.; Park, C. W.; Lee, J. G.; Kim, M. W.; Choi, M. S.; Kim, W. Y.; Yang, J. S.; Yoon, S. S. Supersonically Sprayed Clay, Silica, and Silica Aerogel Hybrid Films as Thermal and Electrical Barriers. *Ceram. Int.* **2018**, *44*, 12934−12939.
(44) Silviana, S.; Sanyoto, G. J.; Darmawan, A. Preparation of Geothermal Silica Glass Coating Film through Multi-Factor Optimization. *J. Teknol.* **2021**, *83*, 41−49.
(45) Silviana, S.; Anggoro, D. D.; Salsabila, C. A.; Aprilio, K. Utilization of Geothermal Waste as a Silica Adsorbent for Biodiesel Purification. *Korean J. Chem. Eng.* **2021**, *38*, 2091−2105.

https://doi.org/10.1021/acsomega.2c03734
ACS Omega 2022, 7, 41968−41980

(46) Silviana, S.; Noorpasha, A.; Rahman, M. M. Preliminary Study of Chitosan Coating Silica Derived from Geotermal Solid Waste. *Civ. Eng. Arch.* **2020**, *8*, 281−288.
(47) Silviana, S.; Ma'ruf, A. Silicon Preparation Derived from Geothermal Silica by Reduction Using Magnesium. *Int. J. Emerg. Trends Eng. Res.* **2020**, *8*, 4861−4866.
(48) Silviana, S.; Sanyoto, G. J.; Darmawan, A.; Sutanto, H. Geothermal Silica Waste as Sustainable Amorphous Silica Source for the Synthesis of Silica Xerogels. *Rasayan J. Chem* **2020**, *13*, 1692−1700.
(49) Feng, Q.; Chen, K.; Ma, D.; Lin, H.; Liu, Z.; Qin, S.; Luo, Y. Synthesis of High Specific Surface Area Silica Aerogel from Rice Husk Ash via Ambient Pressure Drying. *Colloids Surf., A* **2018**, *539*, 399−406.
(50) Huang, R.; Shen, Y.-W.; Guan, Y.-Y.; Jiang, Y.-X.; Wu, Y.; Rahman, K.; Zhang, L.-J.; Liu, H.-J.; Luan, X. Mesoporous Silica Nanoparticles: Facile Surface Functionalization and Versatile Biomedical Applications in Oncology. *Acta Biomater.* **2020**, *116*, 1−15.
(51) Zhang, D.; Xiao, D.; Yu, Q.; Chen, S.; Chen, S.; Miao, M. Preparation of Mesoporous Silica from Electrolytic Manganese Slags by Using Amino-Ended Hyperbranched Polyamide as Template. *ACS Sustainable Chem. Eng.* **2017**, *5*, 10258−10265.
(52) Silviana, S.; Darmawan, A.; Dalanta, F.; Subagio, A.; Hermawan, F.; Milen Santoso, H. Superhydrophobic Coating Derived from Geothermal Silica to Enhance Material Durability of Bamboo Using Hexadimethylsilazane (HMDS) and Trimethylchlorosilane (TMCS). *Materials* **2021**, *14*, 530.
(53) Shi, F.; Liu, J. X.; Song, K.; Wang, Z. Y. Cost-Effective Synthesis of Silica Aerogels from Fly Ash via Ambient Pressure Drying. *J. Non-Cryst. Solids* **2010**, *356*, 2241−2246.
(54) Olawale, O. Bamboo Leaves as an Alternative Source for Silica in Ceramics Using Box Benhken Design. *Sci. African* **2020**, *8*, No. e00418.
(55) Rangaraj, S.; Venkatachalam, R. A Lucrative Chemical Processing of Bamboo Leaf Biomass to Synthesize Biocompatible Amorphous Silica Nanoparticles of Biomedical Importance. *Appl. Nanosci.* **2017**, *7*, 145−153.
(56) Abbas, N.; Khalid, H. R.; Ban, G.; Kim, H. T.; Lee, H. K. Silica Aerogel Derived from Rice Husk: An Aggregate Replacer for Lightweight and Thermally Insulating Cement-Based Composites. *Constr. Build. Mater.* **2019**, *195*, 312−322.
(57) Hu, S.; Hsieh, Y.-L. Preparation of Activated Carbon and Silica Particles from Rice Straw. *ACS Sustainable Chem. Eng.* **2014**, *2*, 726−734.
(58) Kuga, S. The Porous Structure of Cellulose Gel Regenerated from Calcium Thiocyanate Solution. *J. Colloid Interface Sci.* **1980**, *77*, 413−417.
(59) Yang, K. S.; Theil, M. H.; Chen, Y. S.; Cuculo, J. A. Formation and Characterization of the Fibres and Films from Mesophase Solutions of Cellulose in Ammonia/Ammonium Thiocyanate Solvent. *Polymer* **1992**, *33*, 170−174.
(60) Frey, M. W.; Theil, M. H. Calculated Phase Diagrams for Cellulose/Ammonia/Ammonium Thiocyanate Solutions in Comparison to Experimental Results. *Cellulose* **2004**, *11*, 53−63.
(61) Ass, B. A. P.; Belgacem, M. N.; Frollini, E. Mercerized Linters Cellulose: Characterization and Acetylation in N,N-Dimethylacetamide/Lithium Chloride. *Carbohydr. Polym.* **2006**, *63*, 19−29.
(62) Wan, C.; Lu, Y.; Jiao, Y.; Cao, J.; Sun, Q.; Li, J. Cellulose Aerogels from Cellulose-NaOH/PEG Solution and Comparison with Different Cellulose Contents. *Mater. Sci. Technol.* **2015**, *31*, 1096−1102.
(63) Kamal Mohamed, S. M.; Ganesan, K.; Milow, B.; Ratke, L. The Effect of Zinc Oxide (ZnO) Addition on the Physical and Morphological Properties of Cellulose Aerogel Beads. *RSC Adv.* **2015**, *5*, 90193−90201.
(64) Wang, S.; Lu, A.; Zhang, L. Recent Advances in Regenerated Cellulose Materials. *Prog. Polym. Sci.* **2016**, *53*, 169−206.
(65) Lu, L.; Lin, C.; Li, A.; Cao, Y. A Simple and Efficient Approach to Cellulose/Silica Composite Aerogel with High Silica Utilization Efficiency. *J. Res. Updates Polym. Sci.* **2015**, *4*, 56−61.
(66) Demilecamps, A.; Reichenauer, G.; Rigacci, A.; Budtova, T. Cellulose-Silica Composite Aerogels from "One-Pot" Synthesis. *Cellulose* **2014**, *21*, 2625−2636.
(67) Miao, Y.; Pudukudy, M.; Zhi, Y.; Miao, Y.; Shan, S.; Jia, Q.; Ni, Y. A Facile Method for in Situ Fabrication of Silica/Cellulose Aerogels and Their Application in CO2 Capture. *Carbohydr. Polym.* **2020**, *236*, No. 116079.
(68) He, F.; He, X.; Yang, W.; Zhang, X.; Zhou, L. In-Situ Synthesis and Structural Characterization of Cellulose-Silica Aerogels by One-Step Impregnation. *J. Non-Cryst. Solids* **2018**, *488*, 36−43.
(69) Şahin, İ.; Özbakır, Y.; Inönü, Z.; Ulker, Z.; Erkey, C. Kinetics of Supercritical Drying of Gels. *Gels* **2018**, *4*, 3.
(70) Gurav, J. L.; Jung, I.-K.; Park, H.-H.; Kang, E. S.; Nadargi, D. Y. Silica Aerogel: Synthesis and Applications. *J. Nanomater.* **2010**, *2010*, 1−11.
(71) Zuo, L.; Zhang, Y.; Zhang, L.; Miao, Y. E.; Fan, W.; Liu, T.*Polymer/Carbon-Based Hybrid Aerogels: Preparation, Properties and Applications*; 2015; Vol. *8*, DOI: 10.3390/ma8105343.
(72) Maleki, H.; Durães, L.; Portugal, A. Development of Mechanically Strong Ambient Pressure Dried Silica Aerogels with Optimized Properties. *J. Phys. Chem. C* **2015**, *119*, 7689−7703.
(73) Silviana, S.; Hermawan, F.; Indracahya, J.; Kusumawardhani, D. A. L.; Dalanta, F. Optimizing the Environmentally Friendly Silica-Cellulose Aerogel Composite for Acoustic Insulation Material Derived from Newspaper and Geothermal Solid Waste Using a Central Composite Design. *J. Sol-Gel Sci. Technol.* **2022**, 1−8.
(74) Alhajabdalla, M.; Mahmoud, H.; Nasser, M. S.; Hussein, I. A.; Ahmed, R.; Karami, H. Application of Response Surface Methodology and Box-Behnken Design for the Optimization of the Stability of Fibrous Dispersion Used in Drilling and Completion Operations. *ACS Omega* **2021**, *6*, 2513−2525.
(75) Ferreira, S. L. C.; Bruns, R. E.; Ferreira, H. S.; Matos, G. D.; David, J. M.; Brandão, G. C.; da Silva, E. G. P.; Portugal, L. A.; dos Reis, P. S.; Souza, A. S.; dos Santos, W. N. L. Box-Behnken Design: An Alternative for the Optimization of Analytical Methods. *Anal. Chim. Acta* **2007**, *597*, 179−186.
(76) Oh, K. W.; Kim, D. K.; Kim, S. H. Ultra-Porous Flexible PET/Aerogel Blanket for Sound Absorption and Thermal Insulation. *Fibers Polym.* **2009**, *10*, 731−737.
(77) Adhikary, S. K.; Ruzdionis, Ž.; Tučkutė, S.; Ashish, D. K. Effects of Carbon Nanotubes on Expanded Glass and Silica Aerogel Based Lightweight Concrete. *Sci. Rep.* **2021**, *11*, 1−11.
(78) Li, J.; Jiao, Y.; Wan, C. Synthesis of MnFe2O4/Cellulose Aerogel Nanocomposite with Strong Magnetic Responsiveness. *Front. Agric. Sci. Eng* **2017**, *4*, 116−120.
(79) Wan, C.; Lu, Y.; Jiao, Y.; Cao, J.; Sun, Q.; Li, J. Preparation of Mechanically Strong and Lightweight Cellulose Aerogels from Cellulose-NaOH/PEG Solution. *J. Sol-Gel Sci. Technol.* **2015**, *74*, 256−259.
(80) Zhang, T.; Yuan, D.; Guo, Q.; Qiu, F.; Yang, D.; Ou, Z. Preparation of a Renewable Biomass Carbon Aerogel Reinforced with Sisal for Oil Spillage Clean-up: Inspired by Green Leaves to Green Tofu. *Food Bioprod. Process.* **2019**, *114*, 154−162.
(81) Guzun, A. S.; Stroescu, M.; Jinga, S. I.; Voicu, G.; Grumezescu, A. M.; Holban, A. M. Plackett-Burman Experimental Design for Bacterial Cellulose-Silica Composites Synthesis. *Mater. Sci. Eng. C* **2014**, *42*, 280−288.
(82) Ashori, A.; Sheykhnazari, S.; Tabarsa, T.; Shakeri, A.; Golalipour, M. Bacterial Cellulose/Silica Nanocomposites: Preparation and Characterization. *Carbohydr. Polym.* **2012**, *90*, 413−418.
(83) Hospodarova, V.; Singovszka, E.; Stevulova, N. Characterization of Cellulosic Fibers by FTIR Spectroscopy for Their Further Implementation to Building Materials. *Am. J. Anal. Chem.* **2018**, *09*, 303−310.

https://doi.org/10.1021/acsomega.2c03734
ACS Omega 2022, 7, 41968−41980

(84) Poletto, M.; Ornaghi Júnior, H. L.; Zattera, A. J. Native Cellulose: Structure, Characterization and Thermal Properties. *Materials* **2014**, *7*, 6105−6119.
(85) Ramalla, I.; Gupta, R. K.; Bansal, K. Effect on Super-hydrophobic Surfaces on Electrical Porcelain Insulator, Improved Technique at Polluted Areas for Longer Life and Reliability. *Int. J. Eng. Technol.* **2015**, *4*, 509.
(86) Wang, X.; Li, C.; Shi, Z.; Zhi, M.; Hong, Z. The Investigation of an Organic Acid Assisted Sol-Gel Method for Preparing Monolithic Zirconia Aerogels. *RSC Adv.* **2018**, *8*, 8011−8020.
(87) He, M.; Duan, B.; Xu, D.; Zhang, L. Moisture and Solvent Responsive Cellulose/SiO2 Nanocomposite Materials. *Cellulose* **2015**, *22*, 553−563.
(88) Litschauer, M.; Neouze, M. A.; Haimer, E.; Henniges, U.; Potthast, A.; Rosenau, T.; Liebner, F. Silica Modified Cellulosic Aerogels. *Cellulose* **2011**, *18*, 143−149.
(89) Azmi, A.; Lau, K. S.; Chin, S. X.; Khiew, P. S.; Zakaria, S.; Chia, C. H. Zinc Oxide-Filled Polyvinyl Alcohol−Cellulose Nanofibril Aerogel Nanocomposites for Catalytic Decomposition of an Organic Dye in Aqueous Solution. *Cellulose* **2021**, *28*, 2241−2253.
(90) Cai, J. Y.; Lucas, S.; Wang, L.; Cao, Y. Insulation Properties of the Monolithic and Flexible Aerogels Prepared at Ambient Pressure. *Adv. Mater. Res.* **2011**, *391*−*392*, 116−120.
(91) Yan, P.; Zhou, B.; Du, A. Synthesis of Polyimide Cross-Linked Silica Aerogels with Good Acoustic Performance. *RSC Adv.* **2014**, *4*, 58252−58259.
(92) Sachithanadam, M.; Joshi, S. C. Effect of Granule Sizes on Acoustic Properties of Protein-Based Silica Aerogel Composites via Novel Inferential Transmission Loss Method. *Gels* **2016**, *2*, 11.
(93) Merli, F.; Anderson, A. M.; Carroll, M. K.; Buratti, C. Acoustic Measurements on Monolithic Aerogel Samples and Application of the Selected Solutions to Standard Window Systems. *Appl. Acoust.* **2018**, *142*, 123−131.
(94) Navard, P.*The European Polysaccharide Network of Excellence (EPNOE): Research Initiatives and Results*; 2013, DOI: 10.1007/978-3-7091-0421-7.
(95) Purnomo, A.; Dalanta, F.; Oktaviani, A. D.; Silviana, S. *Superhydrophobic Coatings and Self-Cleaning through the Use of Geothermal Scaling Silica in Improvement of Material Resistance*; 2018; p 020077, DOI: 10.1063/1.5065037.
(96) Affandi, S.; Setyawan, H.; Winardi, S.; Purwanto, A.; Balgis, R. A Facile Method for Production of High-Purity Silica Xerogels from Bagasse Ash. *Adv. Powder Technol.* **2009**, *20*, 468−472.
(97) Mazrouei-Sebdani, Z.; Begum, H.; Schoenwald, S.; Horoshenkov, K. V.; Malfait, W. J. A Review on Silica Aerogel-Based Materials for Acoustic Applications. *J. Non-Cryst. Solids* **2021**, *562*, No. 120770.
(98) Garrido, R.; Silvestre, J. D.; Flores-Colen, I.; Júlio, M. d. F.; Pedroso, M. Economic Assessment of the Production of Subcritically Dried Silica-Based Aerogels. *J. Non-Cryst. Solids* **2019**, *516*, 26−34.

https://doi.org/10.1021/acsomega.2c03734
ACS Omega 2022, 7, 41968−41980